In this context, it is necessary to mention that corners were defined as a point of discontinuity of the time derivatives of the space coordinates, but the space coordinates themselves were supposed to be continuous there Thus, Troitskii[3] used the relations,

$$x_s^-(t^*) = x^+(t^*) \qquad \Delta x^-(t^*) = \Delta x^+(t^*)$$

But in this paper we deal with the different assumption that has been explained in the foregoing So, in view of the discontinuity of some or all of the space coordinates at the corner, we use the following relations:

$$x_s^-(t^*) \neq x_s^+(t^*) \qquad \Delta x_s^-(t^*) \neq \Delta x_s^+(t^*)$$

We note here that $\Delta x_i^{\pm}(t^*)$ are independent for $i = 1, \quad n$ and also that δt^*, $(2n - p)$ of the variations δx_{i0} and δx_{i1} and $2(n - m)$ of the variations $\delta x_i^{\pm}$ are independent Therefore, it is possible to select p ν_k's and $2m$ $\lambda_j^{\pm}$'s such that the coefficients of the remaining δx_{i0} and δx_{i1} and $\delta x_i^{\pm}$ in Eq (9) may be zero Thus, in Eq (9), the coefficients of all the variations δt_0, δt_1, δt^*, δx_{i0}, δx_{i1}, $\delta x_i^{\pm}$, $\Delta x_i^{\pm}(t^*)$ must vanish as though they were all independent Hence, we get the following equations from (9):

$$(\partial H/\partial t_0) + (\partial H/\partial x_{i0})\ \dot{x}_{i0} = 0 \tag{10}$$

$$(\partial H/\partial t_1) + (\partial H/\partial x_{i1})\ \dot{x}_{i1} = 0 \tag{11}$$

$$\frac{\partial H}{\partial x_{i0}} - \lambda_j(t_0)\left[\frac{\partial \varphi_j}{\partial \dot{x}_i}\right]_{t_0} = 0 \text{ or } \frac{\partial H}{\partial x_{i0}} - \left(\frac{\partial F}{\partial \dot{x}_i}\right)_0 = 0 \tag{12}$$

$$\frac{\partial H}{\partial x_{i1}} + \lambda_j(t_1)\left[\frac{\partial \varphi_j}{\partial \dot{x}_i}\right]_{t_1} = 0 \text{ or } \frac{\partial H}{\partial x_{i1}} + \left(\frac{\partial F}{\partial \dot{x}_i}\right)_1 = 0 \tag{13}$$

$$\lambda_j^{\pm}\frac{\partial \varphi_j}{\partial x_i^{\pm}} - \dot{\lambda}_j^{\pm}\frac{\partial \varphi_j}{\partial \dot{x}_i^{\pm}} - \lambda_j^{\pm}\frac{d}{dt}\left(\frac{\partial \varphi_j}{\partial \dot{x}_i^{\pm}}\right) = 0$$

$$\text{or} \quad \frac{\partial F}{\partial x_i^{\pm}} - \frac{d}{dt}\left(\frac{\partial F}{\partial \dot{x}_i^{\pm}}\right) = 0 \tag{14}$$

$$\left[\lambda_j^- \frac{\partial \varphi_j}{\partial \dot{x}_i^-}\dot{x}_i^- - \lambda_j^+ \frac{\partial \varphi_j}{\partial \dot{x}_i^+}\dot{x}_i^+\right]_{t^*} = 0$$

$$\text{or} \quad \left[\dot{x}_i^- \frac{\partial F}{\partial \dot{x}_i^-} - \dot{x}_i^+ \frac{\partial F}{\partial \dot{x}_i^+}\right]_{t^*} = 0 \tag{15}$$

$$\left[\lambda_j^{\pm}\frac{\partial \varphi_j}{\partial \dot{x}_i^{\pm}}\right]_{t^*} = 0 \quad \text{or} \quad \left[\frac{\partial F}{\partial \dot{x}_i^{\pm}}\right]_{t^*} = 0 \tag{16}$$

Equations (10–14) are the governing equations of the system and are the same here as in Ref 2 Equations (15) and (16) are the corner conditions The condition in (15) means that $\dot{x}_i(\partial F/\partial \dot{x}_i)$ is continuous across the corner This is identical with the corresponding condition as stated in Ref 2, namely, that $F - \dot{x}_i(\partial F/\partial \dot{x}_i)$ is continuous at the corner ($F \equiv 0$ everywhere)

Equation (16) means that $\partial F/\partial \dot{x}_i$ is continuous through the value zero at the corner The classical corner condition as stated in Ref 2 gives only the continuity of $\partial F/\partial \dot{x}_i$ at the corner, but it does not give the vanishing of this partial derivative on either side of the corner This modification of the corner condition is due to the discontinuity of x_i at the corner and is available only for such space coordinates x_i as are discontinuous there For other space coordinates, only the classical condition of continuity is available, provided their time derivatives are discontinuous A nontrivial application of this modified corner condition is under preparation and may be published soon

References

[1] Bliss, G A , *Lectures on the Calculus of Variations* (University of Chicago Press, Chicago, 1946) Chap VII

[2] Lawden, D F , "Necessary conditions for optimal rocket trajectories," Quart J Mech Appl Math **XII**, 476–487 (November 1959)

[3] Troitskii, V A , "The Mayer-Bolza problem of the calculus of variations and the theory of optimum systems," Prikl Mat Mekh **25**, 668–679 (1961)

Additional Modes of Instability for Poiseuille Flow over Flexible Walls

F D Hains*

Boeing Scientific Research Laboratories, Seattle, Wash

THE modification of Tollmein-Schlichting waves by flexible walls was presented by Hains and Price[1] for two-dimensional Poiseuille flow The possibility of the appearance of other modes of instability was examined by Brooke-Benjamin [2] Using the asymptotic theory, Landahl[3] computed stability diagrams for the Blasius profile This note will compare the stability curves of Refs 1 and 3 and present additional eigenvalues for Poiseuille flow which lead to instability

The stability diagram (Fig 1) shows the modification of Tollmein-Schlichting waves with wall flexibility The stability curves close and the region of instabil ty becomes progressively smaller as the flexibility increases until complete stability results In agreement with the trends given in Ref 2, Landahl[3] found that wall flexibility displaced the stability curve for Tollmein-Schlichting waves to lower wave numbers α and slightly higher Reynolds number R No mention is made of the closing and shrinking of the stability curves

These divergent results are probably due to how the wall properties are nondimensionalized The no-slip condition at the flexible surface leads to the relation

$$\xi(d^3\phi/dy^3) + \phi = 0 \tag{1}$$

which reduces to the condition for a rigid wall when $\xi = 0$ Depending on the free parameter chosen in R, ξ is given by one of the four relations in Table 1 The wall is a membrane stretched with tension T and has a damping coefficient D The nondimensional forms of these quantities are K_3 and K_2, respectively, given in Table 1 The fluid density is ρ, and the viscosity is μ For Poiseuille flow, U_∞ is the maximum velocity, and L is the channel half-width For the Blasius profile, U_∞ is the freestream velocity, and L is the boundary-layer thickness

Hains and Price chose U_∞ as the free parameter, whereas Landahl chose μ Apparently, the latter choice was made in order to obtain a boundary condition that is independent of R The exact boundary condition given by Eq (1) is independent of R if ρ is chosen as the free parameter An approximation to Eq (1) was used in Ref 3 by employing the inviscid equa-

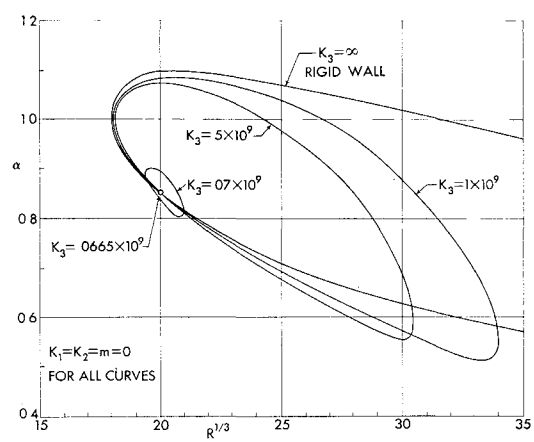

Fig 1 Stability diagrams for the Tollmein-Schlichting mode for Poiseuille flow with walls with increased flexibility Wall damping, mass, and elastic foundation neglected R changed by variation of U_∞ only (from Ref 1)

Received December 24, 1963

* Staff Scientist

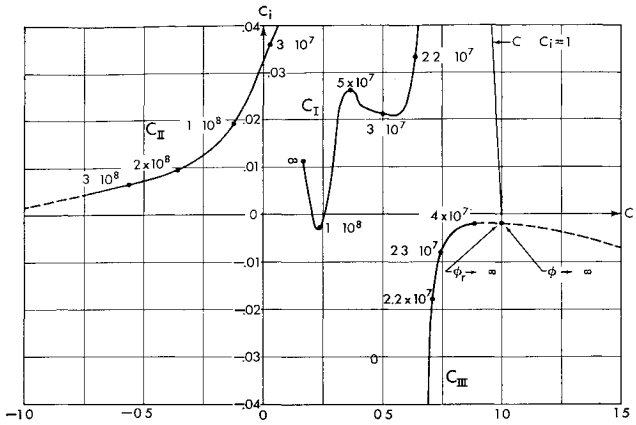

Fig 2 Effect of wall flexibility K_3 on the eigenvalues for Poiseuille flow between flexible walls for $\alpha = 0.6$, $R = (25)^3$

tion to obtain the pressure at the wall It turns out that this approximation is independent of R if μ is chosen as the free parameter Unfortunately, it is customary to interpret the increase in R for the boundary layer on a flat plate as an increase in the freestream velocity or boundary-layer thickness rather than an increase in μ Therefore, a direct comparison of the stability curves of Refs 1 and 3 is not possible To be complete, it is necessary to compute four sets of stability curves each corresponding to one of the four free parameters Presently, calculations are under way to obtain these curves for the Blasius profile

The stability curves in Fig 1 were obtained by numerical solution of the Orr-Sommerfeld equation by a finite-difference technique Values corresponding to Tollmein-Schlichting waves for a rigid wall were used as initial guesses for the eigenvalue c By taking a number of guesses over the entire complex plane, other eigenvalues were found These are shown in Fig 2 for the point $\alpha = 0.6$, $R = (25)^3$

The Tollmein-Schlichting mode C_I is stable ($c_i > 0$) for a rigid wall ($K_3 = \infty$) As the flexibility is increased, this mode first becomes unstable ($c_i < 0$) and then stable again The eigenvalue C_{II} describes waves that travel upstream ($c_r < 0$) when $K_3 > 4 \times 10^7$, stationary waves ($c = 0$) when $K_3 = 4 \times 10^7$, and waves that travel downstream when $K_3 < 4 \times 10^7$ For the range of flexibility shown in Fig 2, this mode is stable, but it appears that unstability will occur as the wall becomes rigid

The third eigenvalue appears to be always unstable For small values of K_3, it is the conjugate of C_I As K_3 increases and c_r approaches one, the eigenfunction ϕ approaches infinity Across this singularity there is a change in sign in the real part of ϕ so that a phase jump of 180° occurs in the velocity components as c_r passes through one Several other eigenvalues were found in the first quadrant along the line $c + c_i = 1$

Preliminary results show that wall damping tends to stabilize C_{II} and C_{III} and destabilize C_I However, very large values of wall damping will stabilize C_I as the wall becomes rigid

The value of $(d^4\phi/dy^4)/\phi(0)$ is usually a maximum at the wall $y = 1$ In the calculation of C_I, it rarely exceeds 5×10^4, but for C_{II} and C_{III}, it can exceed 1×10^6 as indicated by the dashed portions of the curves in Fig 2 Since the third derivation is used in the boundary condition equation (1), the accuracy of the result is reduced as K_3 increases To improve accuracy it was necessary to modify the program used in Ref 1 The truncation error was reduced by taking smaller steps near the wall and a higher-order finite difference approximation for the boundary conditions Unfortunately, roundoff became a problem, so that double precision carrying 16 digits was required The points in Fig 2 were found with the step size $\Delta y = 0.02$ for $0 \leq y \leq 0.7$, and $\Delta y = 0.01$ for $0.7 \leq y \leq 1.0$ Each point required about a minute on an IBM 7090

The values of C_I are accurate to four decimal places and the values of C_{II} and C_{III} to three decimal places, except for the dashed portions of the curves

Table 1 ξ, nondimensionalized damping coefficient K_2, and nondimensionalized tension K_3 as a function of the free parameter in R

Free parameter	$1/\xi$	K_2	K_3
U_∞	$-\left(K_2 + \frac{2}{c}\right)\alpha^2 + i\frac{K_3\alpha^3}{cR}$	$\frac{DL}{\mu}$	$\frac{\rho LT}{\mu^2}$
L	$-\left(K_2R + \frac{2}{c}\right)\alpha^2 + i\frac{K_3\alpha^3}{c}$	$\frac{D}{\rho U_\infty}$	$\frac{T}{\mu U_\infty}$
ρ	$-\left(K_2 + \frac{2}{c}\right)\alpha^2 + i\frac{K_3\alpha^3}{c}$	$\frac{LD}{\mu}$	$\frac{T}{\mu U_\infty}$
μ	$-\left(K_2R + \frac{2}{c}\right)\alpha^2 + i\frac{K_3\alpha^3}{c}R$	$\frac{D}{\rho U_\infty}$	$\frac{T}{L\rho U_\infty^2}$

References

[1] Hains, F D and Price, J F, "Stability of plane Poiseuille flow between flexible walls," *Proceedings of the Fourth U S. National Congress of Applied Mechanics* (American Society of Mechanical Engineers, N Y, 1962) pp 1263–1268

[2] Brooke-Benjamin, T, 'Effects of a flexible boundary on hydrodynamic stability,' J Fluid Mech **9**, 513–532 (1960)

[3] Landahl, M T, "Stability of a boundary layer on a flexible surface,' J Fluid Mech **13**, 609–632 (1962)

Experimental Investigation of Electric Drag on Satellites

EARL D KNECHTEL* AND WILLIAM C PITTS*
NASA Ames Research Center, Moffett Field, Calif

Introduction

ACCURATE knowledge of the satellite drag coefficient is required for predicting satellite lifetime or for determining upper-atmosphere density from orbital decay rates For these purposes, it is generally assumed that the drag is the same as that of an uncharged satellite This assumption is correct at low satellite altitudes where the atmosphere is indeed composed primarily of neutral atoms However, above several hundred kilometers, negative potentials have been measured on satellites, and the relative concentration of ions is known to increase rapidly with altitude Under these conditions, there will be a drag component due to interaction between the satellite charge and the ambient ions which is called electric drag Several theories have been published which attempt to estimate electric drag However, because of the different assumptions used, the results of the theories differ by orders of magnitude The purpose of the present experimental investigation was to determine the magnitude of the electric drag of conducting spheres and to establish which of the various assumptions used in the theories are plausible The related problem of induction drag due to the earth's magnetic field was not considered in the investigation because of the added experimental complexity However, from calculated values of induction drag, and because of the scaling relations involved, the magnetic effects are

Presented as Preprint 64-32 at the AIAA Aerospace Sciences Meeting, New York, January 20–22, 1964

* Research Scientist